HIGH WALL THICKNESS DLSAW PIPES FOR SOUR SERVICE APPLICATION BY JCOE PROCESS

T.S. Kathayat[1], P.K. Mukherjee[1], R.K. Goyal[1], J.R. Shant[1] and R. Hill[2]

[1]WCL Welspun Corp Ltd
[2]Technical Consultant to Welspun
Welspun City, Survey No. 665, Village-Varsamedi, Taluka-Anjar, District-Kutch, Gujarat-370110, India

Keywords: Linepipe, Steelmaking, Sour Service, Heavy Wall Pipe, JCOE Linepipe Process, HIC, NACE, SAW, Offshore, X65, Welding, Mechanical Properties, Microstructure, Charpy Toughness, Hardness

Abstract

Increasing demand in oil and gas supply has increased the number of pipeline installations for offshore and sour service applications. Projects demand higher resistance to H_2S corrosion because of the higher sulfur content observed in the geographical locations. Welspun took a challenging initiative in developing a thick wall forming process with optimized dimensional properties for offshore sour service pipeline application. This paper reports on the manufacturing of API5LX65MSO/L450MSO PSL2 (36"OD x 42.90 mm WT) pipe utilizing the JCOE process at Welspun Pipes Mill in Dahej-Gujarat-India. Special precautions were taken during manufacturing to improve the weld and HAZ properties with respect to toughness at low testing temperatures and control of the pipe manufacturing process without affecting the HIC performance. Selection of plates was considered with respect to alloy design, cleanliness and mechanical properties of both plate and pipe so as to meet the stringent requirements for HIC, hardness, CVN and DWTT as per the client specification. Plates were supplied by voestalpine Grobblech GmbH-Austria. The levels of S<0.0009% and P<0.008% with low values of (Nb+V+Ti)<0.065%, Pcm<0.15% and CE<0.35% were obtained in the TMCP plates. Ultra fine homogeneous ferrite microstructure throughout the thickness has been a great help in pipe forming resulting in improved mechanical properties and excellent HIC test results for plate and pipe. JCO forming and mechanical pipe expansion process parameters were controlled within a narrow range to optimize the pipe dimensional properties such as local and global out-of-roundness in the finished pipes having a low D/t ratio (~21). Hardness and CVN in weld metal and HAZ have been controlled by proper selection of welding consumables, uniform and effective heating of flux, good control of welding parameters and pre-heating of pipe edges before ID welding.

Introduction

Stringent environmental conditions involved in the field of offshore pipelines led to the development of thick wall API5LX65MSO pipes. It is very difficult to achieve satisfactory HIC test results in thick wall plate and pipe having a low D/t ratio (~21) and a consequent large cold forming strain as there are several pipe manufacturing steps which develop stresses which may affect the HIC resistance. The pipe manufacturing process must be controlled by selecting the proper radii of crimping tools, edge mill bevel angle and the radius of the JCO forming tool and the number of strokes. The pipe opening gap after complete forming is minimized before entering the continuous tack welding station. The manufacturing process of

36”OD x 42.90 mm WT pipe using JCOE manufacturing technology is discussed in this paper.

The focus, both in pipe manufacturing and selection of plates, was on the HIC qualification of pipes to withstand high H_2S levels found in certain sea bed locations. Plates (42.90 mm thick x 2712 mm wide) having increased HIC resistance, high impact toughness and uniform microstructural properties were supplied by voestalpine Austria. The lean alloy design selected for the plates resulted in a microstructure mainly consisting of ultra fine ferrite.

Welspun took a challenging initiative to develop heavy wall sour service pipes (36”OD x 42.90 mm WT, API5LX65MSO/L450MSO PSL2), Figure 1, having enhanced HIC resistance and good toughness values both in the HAZ and weld. This was made possible by proper selection of plate chemical composition, welding consumables, stringent control over process parameters starting from pipe forming, submerged arc welding and the testing methods.

Figure 1. Thick wall sour service pipe.

Variables Affecting the HIC Test

Environmental Variables

The important environmental variables are pH, chloride content, temperature, H_2S concentration, presence of dissolved oxygen and the exposure time [1]. Lower pH environments accelerated corrosion as well as stepwise cracking (SWC) [1]. They also demonstrated that a higher concentration of dissolved chlorides increased the severity of the environment [2]. The extent of hydrogen damage was found to be at a maximum in the temperature range of 15 to 35 °C [1]. The sharp reduction in SWC at temperatures above 35 °C is attributed to the decreased concentration of H_2S in the saturated solutions [1].

Metallurgical Variables

Deoxidation practice during casting leads to increased SWC sensitivity; fully-killed steels are almost always more susceptible to HIC as compared to semi-killed steels of a similar composition [1,3]. The susceptibility of steels to HIC depends on sampling location in relation to the cast slab; generally HIC is most prominent in highly segregated regions of the slab [3]. No definite differences were found in HIC resistance attributed to the casting mode

including both continuously cast and ingot cast steel [3]. Microstructural banding (pearlite or martensite) has also been found to increase crack propagation [1].

Restricting the segregation zone hardness to below 300 HV 10 is needed to eliminate HIC degradation since hard "banded" structures of bainite or martensite are susceptible to hydrogen embrittlement as well as HIC [1]. There are different theories about the behavior of welds and HAZ in sour environments [3]. According to one of the theories, sour gas pipeline failures by HIC were always located near spiral welds but never connected with weld defects of any kind [3]. Other researchers have also reported that weld metal, with its dendritic microstructure and oxide inclusions dispersed in the form of fine globules, has excellent resistance to HIC [3].

Stress Variables

A correlation has not yet been established between steel strength and SWC susceptibility [1]. HIC has been reported for a wide range of tensile strengths (300 to 800 MPa) [1]. Internal stresses help the formation of micro-cracks that behave as trapping points and increase the absorption of hydrogen atoms [3].

It seems that nonmetallic inclusions and anomalous microstructures are more important factors in determining HIC susceptibility as compared to the strength of the steel [1]. The SWC mechanism involves segregation of hydrogen atoms to internal interfaces followed by de-cohesion at those interfaces possibly caused by hydrogen pressurization [1]. The plastic regions generated at the blister crack tips are embrittled by hydrogen and transverse cracks propagate through the embrittled regions to join parallel cracks thus giving the appearance of steps [1,3]. SWC occurs not only in unstressed components, but also in steels under elastic tensile stresses [1].

Chemical Variables

The addition of copper has been found beneficial to SWC resistance of linepipe steels [1]. Similarly chromium additions were also found to improve SWC resistance [1]. Beneficial effects of chromium and nickel in reducing hydrogen absorption from sour environments has been observed [1]. Researchers have found that cobalt, bismuth and rhodium additions cause a decrease in hydrogen absorption by steels from H_2S containing environments [1].

Plate Properties

Alloy Design for Plate. The chemical composition, Table I, is of vital importance to withstand high sulfur and H_2S levels and the severe environmental conditions which prevail during transportation of untreated gas/liquid through offshore pipelines.

Table I. Chemical Composition of Plates, wt.%

C	**Si**	**Mn**	**P**	**S**	**Al**	**Cr**	**N**
0.031	0.323	1.53	0.007	0.0006	0.033	0.187	0.004
Ca	**CE**	**Pcm**	**Nb+V+Ti**	**Al/N**			
0.001	0.327	0.13	0.058	8.291			

State-of-the-art technology developed by voestalpine Grobblech GmbH, Austria, for hot rolling (TMCP) of plates is taking advantage of niobium for the development of ultra fine ferrite grains in the microstructure across the full plate thickness, Figure 2. Carbon was maintained at a very low level to utilize the full potential of niobium in grain refinement rather than precipitation of Nb (C,N). This allows one to keep the niobium at lower levels without compromising the strength. An addition of chromium is beneficial in developing a quasi-polygonal ferrite structure which is good for producing a homogeneous strength across the plate thickness.

(a) Steelmaking

(b) Slab Casting

(c) Plate Rolling

(d) Accelerated Cooling

(e) Laminar Cooling

Figure 2. (a – e) Steelmaking, Casting, Rolling and Cooling Facilities at voestalpine.

Plate - Mechanical, Toughness and Hardness Properties

Plate properties are shown in Table II.

Table II. Plate - Mechanical, Toughness and Hardness Properties

	Mechanical Properties (Transverse - Round Bar)				**Impact Toughness (Transverse)**	**Hardness**
Statistics	**YS (0.5%) MPa**	**UTS MPa**	**Elongation at 2" GL %**	**YS/UTS**	**CVN impact at -23 °C 10 x 10 x 55 mm and 2 mm sub-surface (J)**	**Average of 3 values across thickness HV 10 kg**
As per MPS**	440-560	535-655	28 min	0.90 max	Min Ind 175, Min Avg 190	220 max
Min	465	556	32	0.83	438	188
Max	508	573	34	0.89	452	198
Mean	482	562	33	0.86	445	193
Stdev	14	6	0.6	0.02	5	3.8
CoV, %	2.9	1.1	1.7	2.0	1.1	2.0
**MPS: Manufacturing Procedure Specification						

- DWTT SA impact fracture area: minimum individual 85% and minimum average 90%.
- CVN (Subsize-Transverse) at -10 °C = Minimum individual 100% and minimum average 100%.

The plate hardness was measured as shown in Figure 3. The variation of hardness across the plate thickness is shown in Figure 4. The maximum variation across the plate thickness is 11 HV 10 kg which is quite a narrow range and good for HIC resistance.

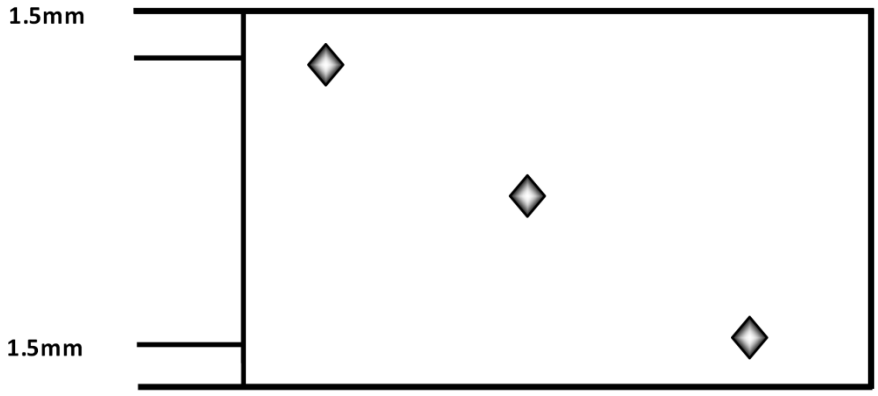

Figure 3. Schematic diagram for hardness measurement.

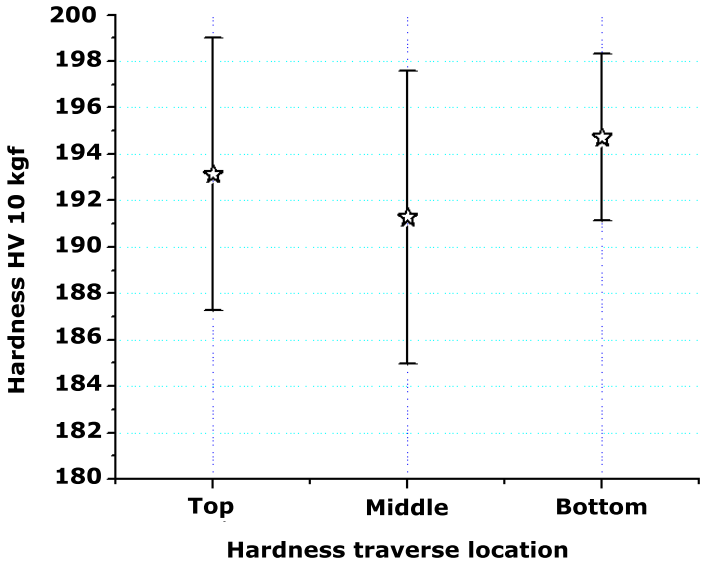

Figure 4. Hardness variation across the plate thickness.

HIC Test Results

Test Procedure

Three coupons were cut from the top end of each test plate. Degreasing of specimens was done as per ASTM F21:65. Three sections of each coupon were evaluated and the values of CLR, CSR and CTR were determined. Sectioning was done at 3 equivalent distances as shown in Figure 5. Pictures were taken with a Zeiss Observer or a Leica Mef-Microscope.

A controlled sample for demonstrating HIC cracking sensitivity was used for the test. The average crack length ratio (CLR) shall exceed 20% in solution "A" after testing of the controlled sample. Control samples of grade S355J2 were used. A control sample is used to check the HIC solution is working efficiently or not and it is checked by crack length ratio obtained being more than 20%. Table III provides a summary of HIC test parameters and Table IV provides a summary of HIC test results.

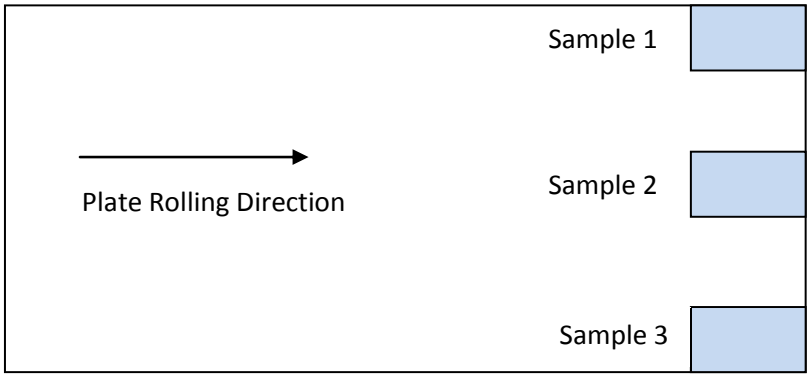

Figure 5. Plate sampling location.

Table III. Summary of HIC Parameters-Plate Samples

Specifications	NACE TM0284:2003: Testing Standard ASTM F21:65: To check whether sample has been degreased or not before test. 01-SAMSS-035:2011, Saudi Aramco Form - 175-010210: Specification		
No. of Setup	**1**	**2**	**3**
Test Solution	Solution A	Solution A	Solution A
Test Temperature, °C	25 ± 3	25 ± 3	25 ± 3
Test Duration, h	96	96	96
Start pH of Solution	2.7	2.7	2.7
Initial pH of Solution after Saturation	3.2	3.2	3.2
Final pH of Solution	3.8	3.8	3.8
Initial H_2S Concentration, ppm	2727	2880	2804
Final H_2S Concentration, ppm	2821	2608	2804
Sample Size (T x W x L), mm	30 (±1) x 20 (±0.5) x100 (±0.5)	30 (±1) x 20 (±0.5) x100 (±0.5)	30 (±1) x 20 (±0.5) x100 (±0.5)
Control Sample Size (T x W x L), mm	19.61 x 20.02 x 100	19.94 x 20.01 x 100	19.99 x 20.02 x 100
Control Sample CLR, %	31	37	78

Table IV. Summary of HIC Test Results

Serial No.	**No. of Heats**	**No. of Plates**	**CLR %**	**CSR %**	**CTR %**
Specification			**10% max**	**1% max**	**3% max**
1	5	5	0	0	0
2	1	1	0.30	0	0.01
3	1	1	0.54	0	0.03

Pipe Production

Pipe production was carried out in various stages from plate to pipe. Challenges were mainly in deforming thick plate into pipe with low dimensional variance along the axial and radial directions. A higher dimensional stability helps in attaining lower residual stress which is beneficial for sour service application.

Figure 6 shows the pipe making stages carried out at Welspun Corp Ltd. The JCO process is accomplished by pipe forming with folding sword in 35 strokes. Expansion was aimed in the range of 0.9% to 1.0% in order to attain close dimensional tolerances.

Crimping Press

The longitudinal edges of plates are trimmed by edge milling to bring the width to the exact required value. Simultaneously, the edges are beveled to form a double "V" groove to accommodate the welding. The first forming step involves crimping of the edges of the plate into a circular arc over a width about one radius on each side. This is achieved by pressing the ends between two shaped dies as per Figure 6(d).

JCO Pipe Forming

The crimped plate moves next to the forming process where JCO forming starts from one longitudinal end of the plate in gradual forming steps to form a J-shape. The process is repeated from the other longitudinal end to form a C-shape. Finally the pipe is converted into an O-shape as shown in Figure 6(e).

Continuous Tack Welding

After JCO pipe forming, the pipe moves to the next station for continuous tack welding from the outside to close the opening gap of the pipe, Figure 6(g). Table V shows the process parameters of the continuous tack welding process.

(a) Plate Inspection

(b) Plate UT

(c) Edge Milling

(d) Edge Crimping

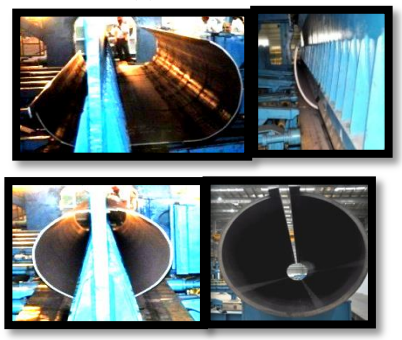

(e) JCO

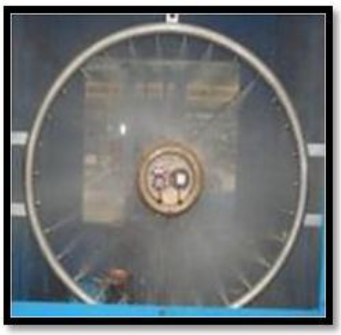

(f) Pipe Washing

(g) Continuous Tack Welding

(h) ID SAW

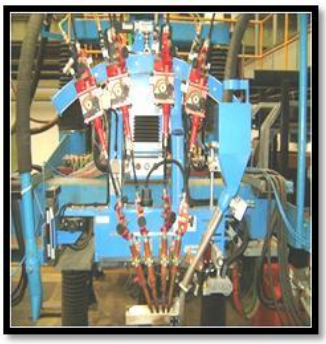

(i) OD SAW

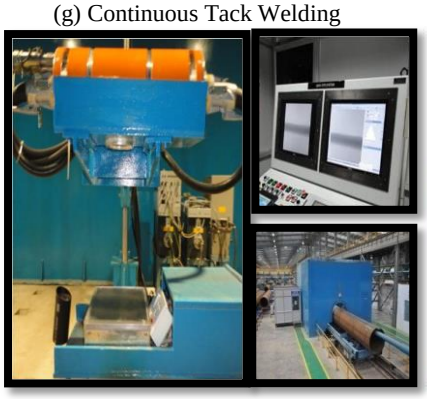

(j) Real Time Radiography

(k) Mechanical Expansion

(l) Hydrostatic Testing

(m) Weld Seam UT

(n) MPI of Bevel Surface

(o) Final Inspection

Figure 6. Stages of pipe production from plate to pipe (a to o).

Table V. Welding Parameters at Tack, ID and OD Welding Stations

	Head	Wire	A	V	Speed (m/min)	S.O. (mm)	Angle	H.I. (kJ/mm)
CONTINUOUS TACK WELDING	DC	ER70S6	900	23.5	2.6	20	0°	0.49
Bevel angle = 30° Upper bevel = 14.9 mm Root face = 13.0 mm Lower bevel = 15.0 mm	Inner Diameter Submerged Arc Welding (ID SAW)							
	DC	EG	1050	34	0.6	38	12°	3.57
	AC1	EG	950	37	0.6	39	0°	3.52
	AC2	EM12K	850	38	0.6	40	15°	3.23
	Flux 995N					Wire diameter: 22-24 mm		10.32
Bevel angle = 30° Upper bevel = 14.9 mm Root face = 13.0 mm Lower bevel = 15.0 mm	Outer Diameter Submerged Arc Welding (OD SAW)							
	DC	EG	1150	34	0.56	37	10°	4.19
	AC1	EG	900	36	0.56	38	0°	3.47
	AC2	EG	800	37	0.56	39	12°	3.17
	Flux 995N					Wire diameter: 19-21 mm		10.83
S.O.: Stickout Length; A: Ampere, V: Voltage; H.I.: Heat Input								

ID and OD Welding

Submerged arc welding of the pipes was performed with Lincoln 995N flux (F9A2) in combination with EG and EM12K wires to achieve the optimized heat input level in order to get the required penetration. As the carbon equivalent was on the low side, without Mo in the plates, better microstructure control was obtained with respect to hardness variation from base and weld. Narrow gap welding, Figure 7, was selected along with a preheat temperature of 100 °C and inter-pass temperature of 95 °C to achieve sound welding without any hydrogen entrapment. Table V shows the welding parameters for ID and OD welding.

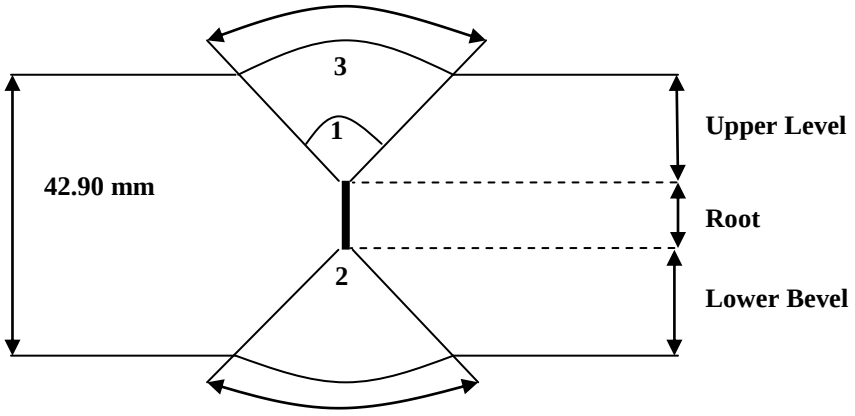

Figure 7. Narrow gap welding pass sequence.

Real time radiography (RTR) was carried out after ID and OD welding to check the weld quality for any discontinuities, however, no defects were observed in the weld seam during RTR as shown in the photographs in Figure 8.

Figure 8. Photographs of real time radiography of weld seam.

Mechanical Properties

Table VI presents the plate and pipe mechanical properties. The coefficient of variation (CoV) did not change much from plate to pipe. The average values of both YS and UTS increased in the pipe from plate by ~30 MPa (~6%) and this is due to plastic deformation during the JCO and mechanical expansion operations. The difference in elongation values is due to different specimen shapes used in plate (round bar) and pipe (flat strip).

Table VI. Plate and Pipe Mechanical Properties

	Plate mechanical properties (Round bar-Transverse)				**Pipe mechanical properties (Flat strip-Transverse)**			
Statistics	**YS (0.5%) MPa**	**UTS MPa**	**Elongation at 2" GL %**	**YS/UTS**	**YS (0.5%) MPa**	**UTS MPa**	**Elongation at 2" GL %**	**YS/UTS**
MPS**	**440-560**	**535-655**	**28 min**	**0.90 max**	**450-570**	**535-760**	**24 minimum**	**0.93 maximum**
Min	465	556	32	0.83	495	577	55	0.84
Max	508	573	34	0.89	535	612	62	0.91
Average	482	562	33	0.86	518	590	59	0.88
Stdev	14	6	0.6	0.02	15	11	2.5	0.02
CoV, %	2.9	1.1	1.7	2.0	2.8	2.0	4.2	2.4
**MPS: Manufacturing Procedure Specification.								

Table VII presents the impact toughness properties in plate and pipe. The fracture surface shear area on broken impact specimens was 100% in both plate and pipes. Charpy impact values in plate and pipe are well above the specification limit. However, the variation in the impact values is due to the change in specimen dimensions and the strain hardening effect. (Subsize Charpy impact specimens were used to test the pipe material). The transverse DWTT shear area was 100% in plate at -10 °C and at -17 °C in the pipe base metal against the specification requirement of a minimum of 75% individual and 85% average at -17 °C in pipe, Figure 9. This indicates that the energy required for crack propagation is similar and that the stresses generated during pipe forming did not alter the fracture resistance.

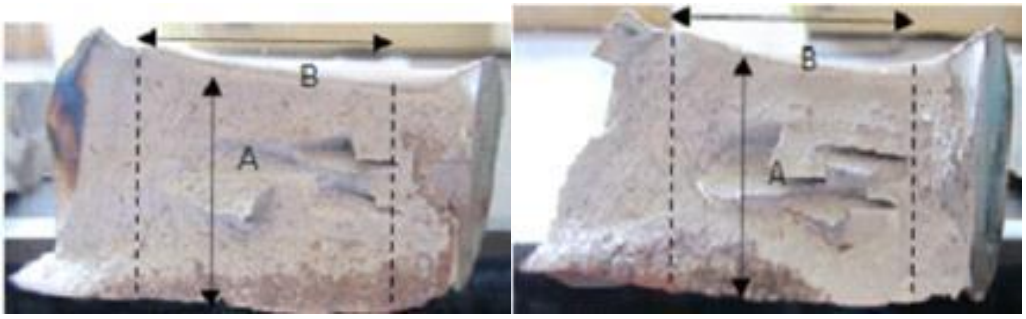

Figure 9. DWTT Shear area in pipe at -17 °C (Reduced size).

% Shear Area: $\frac{(71-2t)t-\frac{3}{4}(AB)}{(71-2t)t}$ (% Shear Area Calculations as per API 5L R3:1996)

A: The width of the cleavage fracture at the "one t" line beneath the notch, mm.

B: The length of the cleavage fracture in between the "two t" lines, mm.

Table VII. Plate and Pipe Toughness Properties

	Transverse base-plate	Transverse base-pipe
	CVN impact energy at -23 °C, (J)	CVN impact energy at -16 °C, (J)
MPS**	**Min Ind 175, Min Avg 190**	**Min Ind 80 and Min Avg 106 (For full size specimen)**
Size	10 x 10 x 55 mm	7.5 x 10 x 55 mm
Min	438	323
Max	452	336
Mean	445	328
Stdev	5	4
CoV, %	1.1	1.2
**MPS: Manufacturing Procedure Specification		

Hardness Profile of Pipe

The hardness was measured as per the schematic diagram in Figure 10, from base metal to weld to base metal. The average variation in hardness from base metal to HAZ is 20 HV and from base metal to weld metal is 40 HV, as shown in Figure 11.

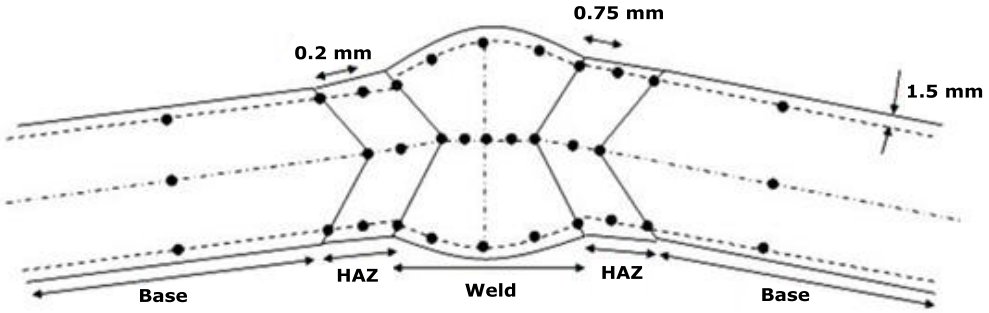

Figure 10. Schematic diagram for hardness measurement.

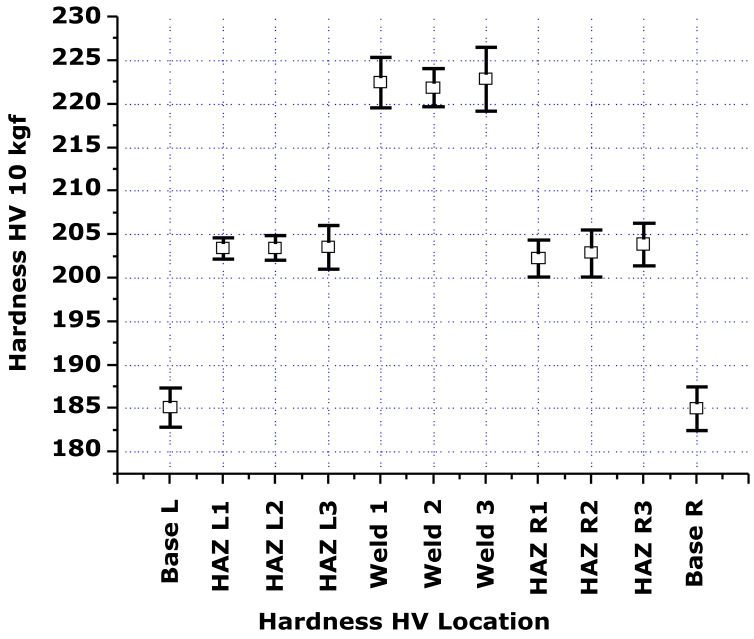

Figure 11. Hardness profile of base-HAZ-weld.

Variation in the hardness is due to the change in grain morphology and phase from fine polygonal ferrite in the base metal to intergranular acicular ferrite in the weld metal as shown in Figure 12. Minimal hardness variation and the presence of acicular ferrite in the weld and coarse acicular ferrite laths in the HAZ leads to good toughness as well as good HIC test results.

The hardness variation across the thickness in both plate and pipe base material is shown in Figure 13. The maximum increase of hardness from plate to pipe was 3 HV 10 kg. This indicates that the stress and strain development during the various stages of pipe manufacturing was well controlled.

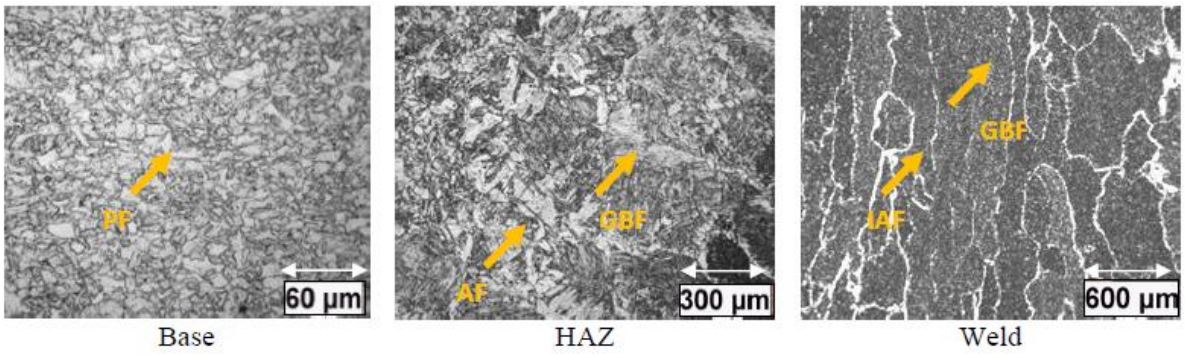

Figure 12. Microstructure variation from base metal to HAZ to the weld.

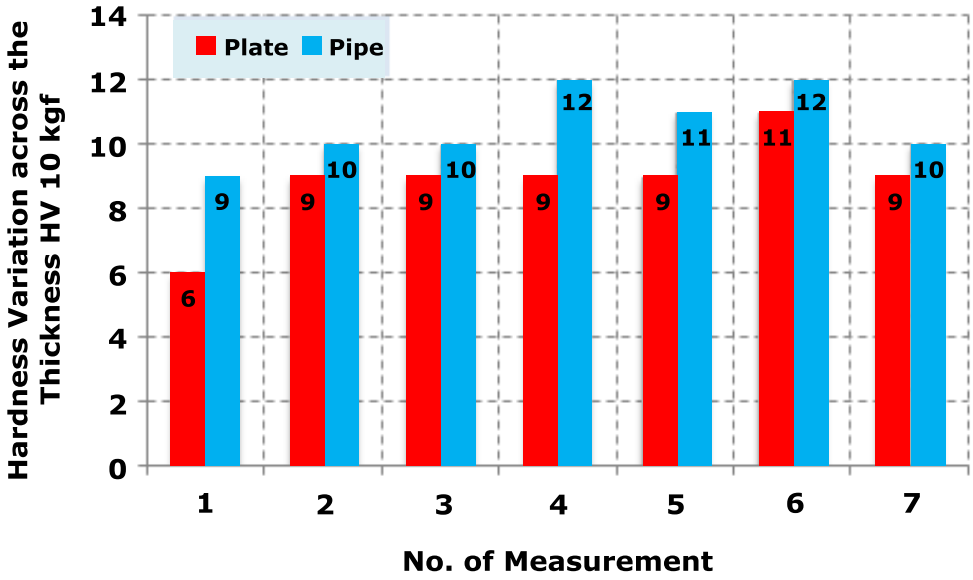

Figure 13. Hardness variation across the thickness in plate and pipe (base material).

Impact Toughness

The percent CoV increased from base to HAZ to weld due to the degree of microstructural inhomogeneity increasing in the same order. The CVN energy values attained in the HAZ and weld are much higher than the specification requirement shown in Table VIII.

Table VIII. Charpy Impact Values (J) of the Pipe at Different Locations

Location	**Base-transverse**		**Fusion line (HAZ)-transverse**		**Weld-transverse**	
	Individual	**Average**	**Individual**	**Average**	**Individual**	**Average**
Temp	At -16 °C		At -13 °C		At -13 °C	
Size	7.5 x 10 x 55 mm		10 x 10 x 55 mm		10 x 10 x 55 mm	
Spec	**Individual 80J min and Average 106J min (For full size specimen)**					
Min	319	323	326	367	108	122
Max	338	336	467	447	213	201
Mean	328	328	426	426	160	160
Stdev	5	4	31	28	25	24
CoV, %	1.7	1.2	7.2	6.6	15.7	14.8

Microstructure Characteristics for Offshore Pipeline

The base metal microstructure shows fine polygonal ferrite grains free from pearlitic bands. The grain size observed in the base metal is predominantly in the range ASTM 12-14, Figure 14. Weld metal shows acicular ferrite with grain boundary ferrite, Figures 15 and 16.

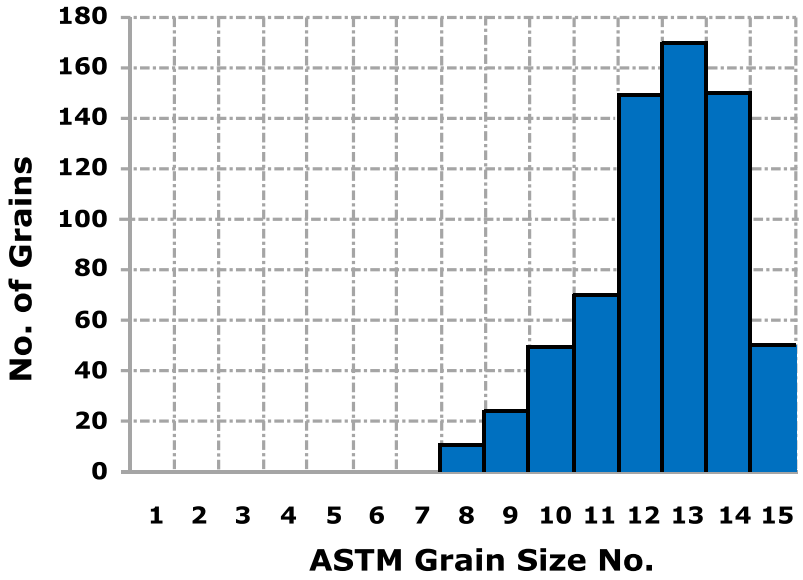

Figure 14. Grain size distribution in base metal.

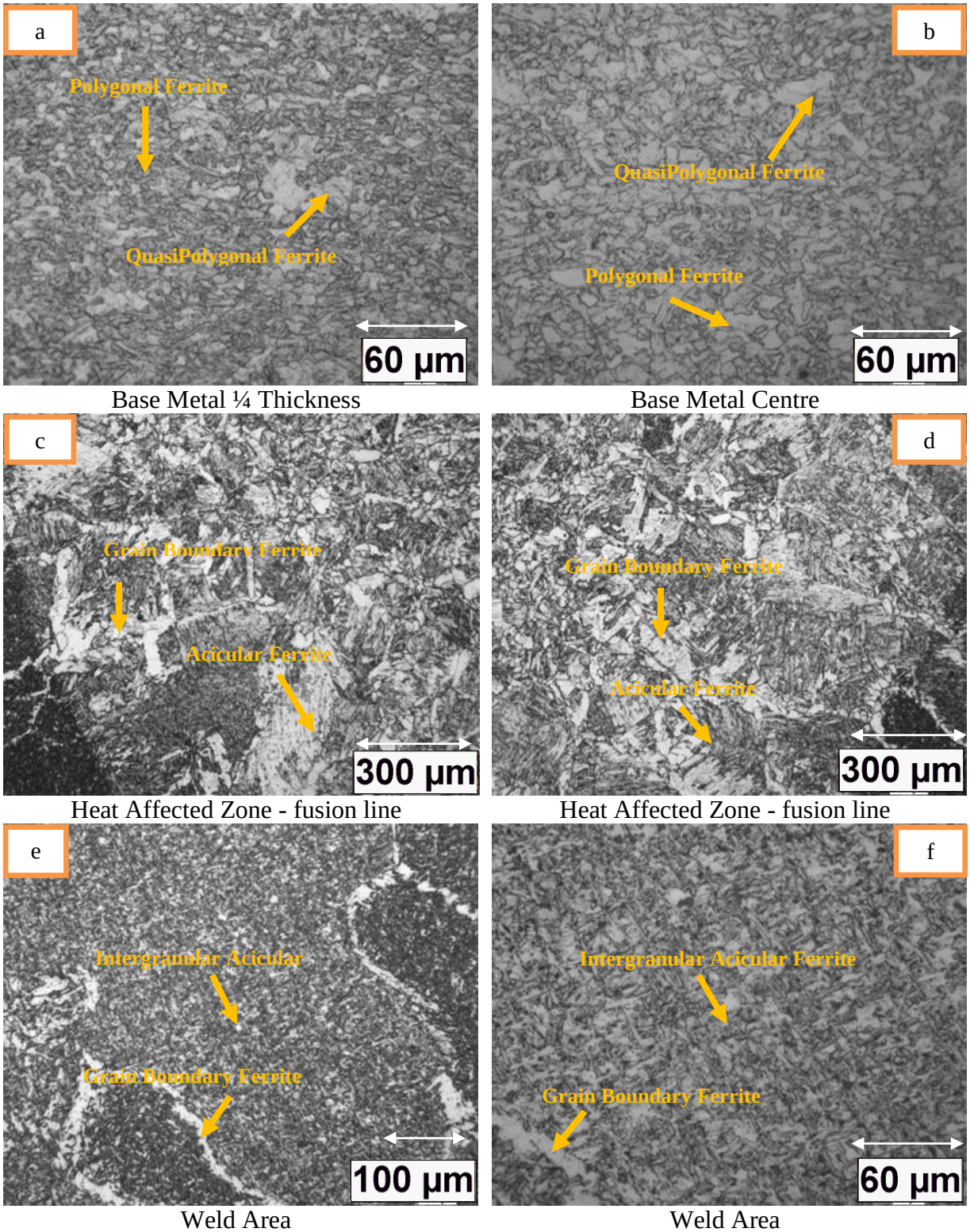

Base Metal ¼ Thickness | Base Metal Centre

Heat Affected Zone - fusion line | Heat Affected Zone - fusion line

Weld Area | Weld Area

Figure 15. Microstructures showing various phases in base metal, heat affected zone and weld region.

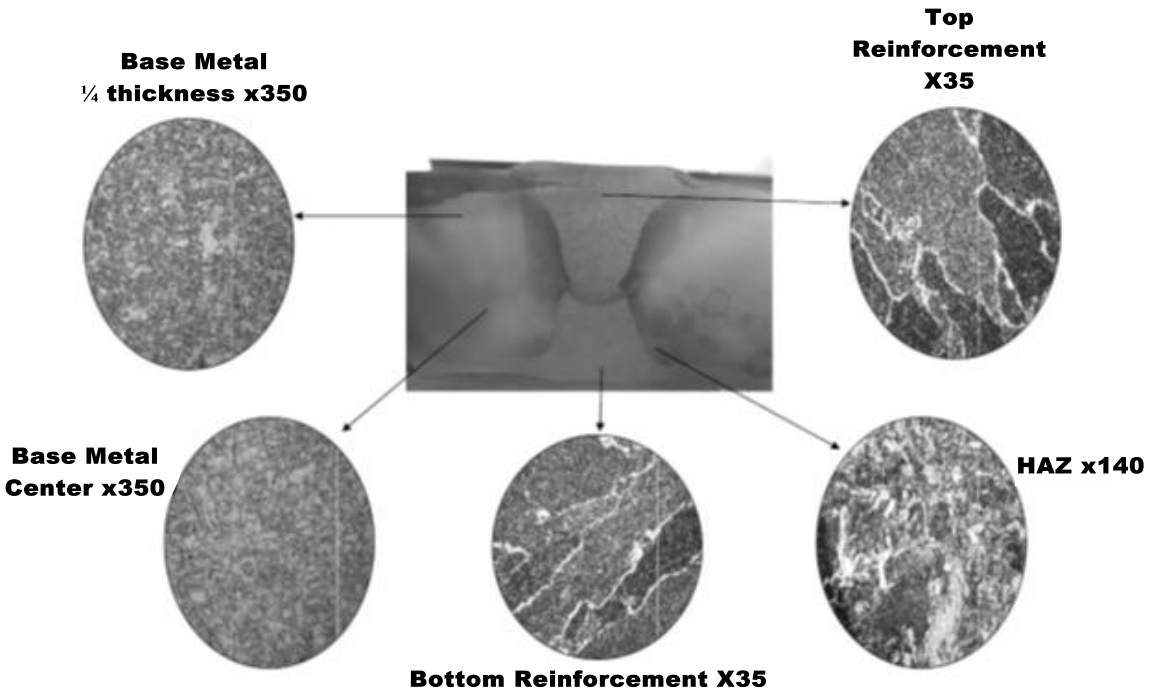

Figure 16. Microstructure of as-welded X65 sour resistant pipe showing base metal and weld microstructure.

Hydrogen Induced Cracking/Step-wise Cracking

HIC testing was carried out as per the specifications 01-SAMSS-035 with NACE TM0284 Solution A. The tests were carried out on standard HIC samples (100 mm x 20 mm x thickness) at 25 °C for 96 h, Figure 17.

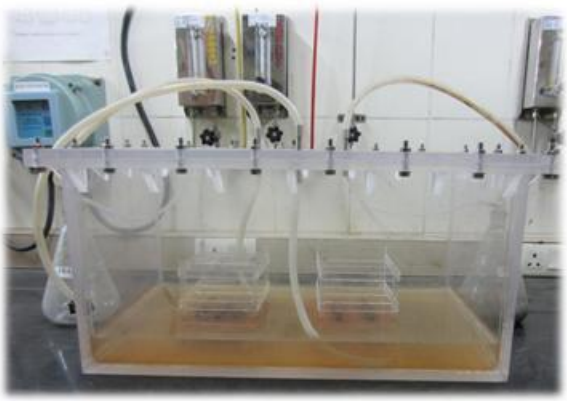

Figure 17. HIC/SWC test setup.

The test solution, containing 0.5% acetic acid and 5% sodium chloride dissolved in distilled water, was saturated with H_2S. The initial and final pH values of the solution were 2.7 and 3.7 respectively. After the test, the three polished metallographic sections from each sample were ultrasonically inspected for cracks. For each section, three different cracking parameters were measured according to Equations (1-3) below. The HIC susceptibility values of CLR, CTR and CSR for each sample were the average of three sections:

$$\text{Crack Length Ratio: CLR} = \frac{\sum a}{W} \times 100\% \quad (1)$$

$$\text{Crack Thickness Ratio: CTR} = \frac{\sum b}{T} \times 100\% \quad (2)$$

$$\text{Crack Sensitivity Ratio: CSR} = \frac{\sum(axb)}{WXT} \times 100\% \quad (3)$$

where 'a' is the crack length in mm, 'b' the crack thickness in mm, 'W' the section width in mm and 'T' the test specimen thickness in mm.

HIC testing was carried out on both plate and pipe to analyze the effect of the pipe manufacturing process on HIC test results. However, the values of CLR, CSR and CTR were found to be the same in both plate and pipe, Table IX. Further studies were carried out on the samples in the laboratory with the help of immersion ultrasonic testing, Figure 18, using C-Scan to check for fine cracks before and after HIC testing as shown in Figure 19. HIC testing was carried out across base metal, HAZ and weld where the results were found to be similar before and after HIC testing, Figure 20.

Table IX. HIC Micro Samples of Pipe at 90°, 180° and Across the Weld

No. of tests	**Location**	**CLR % (Avg.)**	**CSR % (Avg.)**	**CTR % (Avg.)**
		Spec -10% max.	**Spec - 2% max.**	**Spec - 3% max.**
5	90° from weld	0.00	0.00	0.00
	180° from weld	0.00	0.00	0.00
	Across the weld	0.00	0.00	0.00
1	90° from weld	**0.89**	0.00	0.00
	180° from weld	0.00	0.00	0.00
	Across the weld	0.00	0.00	0.00
2	90° from weld	0.00	0.00	0.00
	180° from weld	0.00	0.00	0.00
	Across the weld	**0.40**	0.00	0.00
CSR = Crack Sensitivity Ratio, CLR = Crack Length Ratio, CTR = Crack Thickness Ratio				

Figure 18. Immersion ultrasonic testing setup from GE Energy Inspection Technologies.

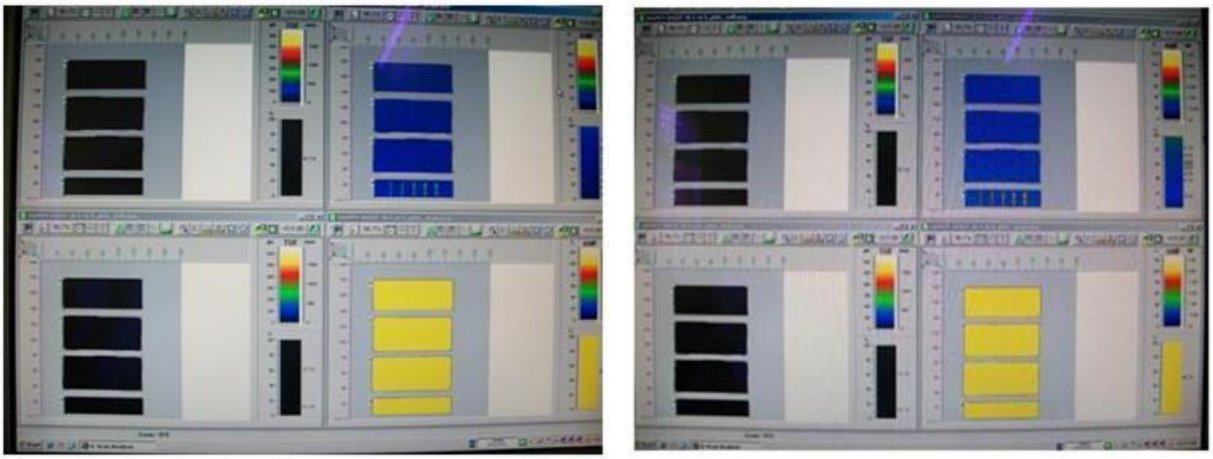

C Scan Before HIC C Scan After HIC

C Scan before and after shows same because no crack was observed in the sample after HIC test

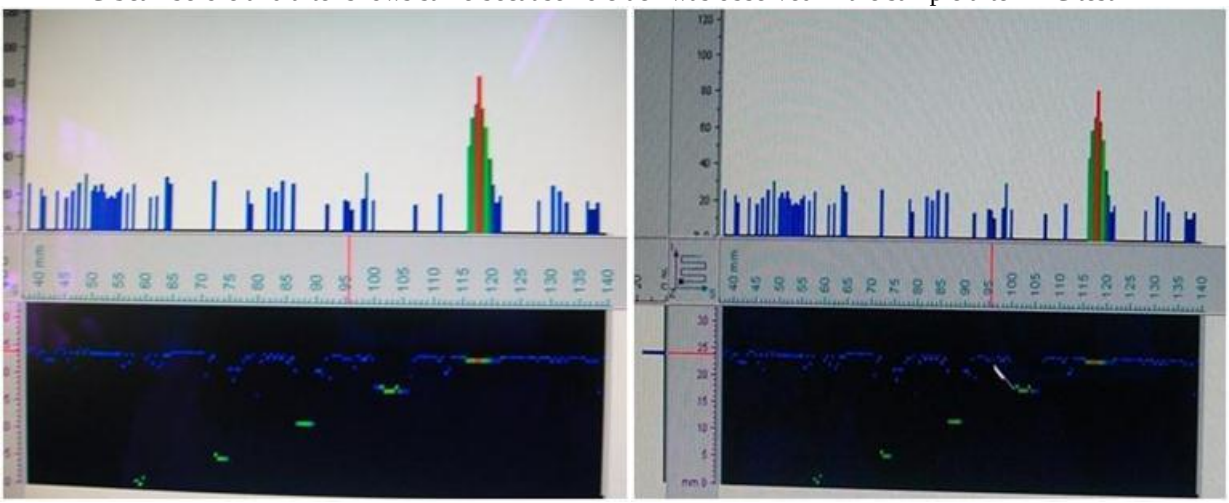

B Scan Before HIC B Scan After HIC

Figure 19. Samples under UT scan before and after HIC samples.

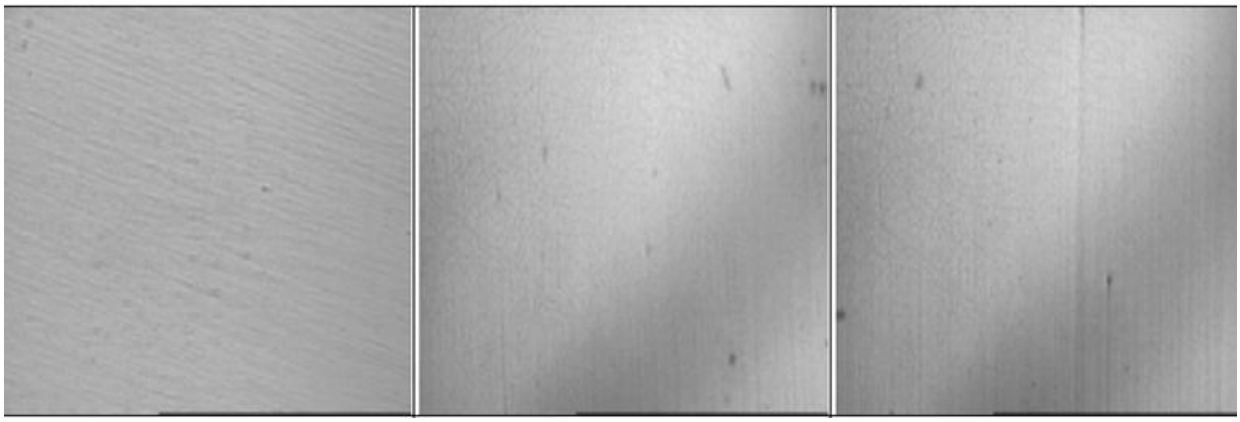

3 sections of pipe sample 90° from the weld; x70

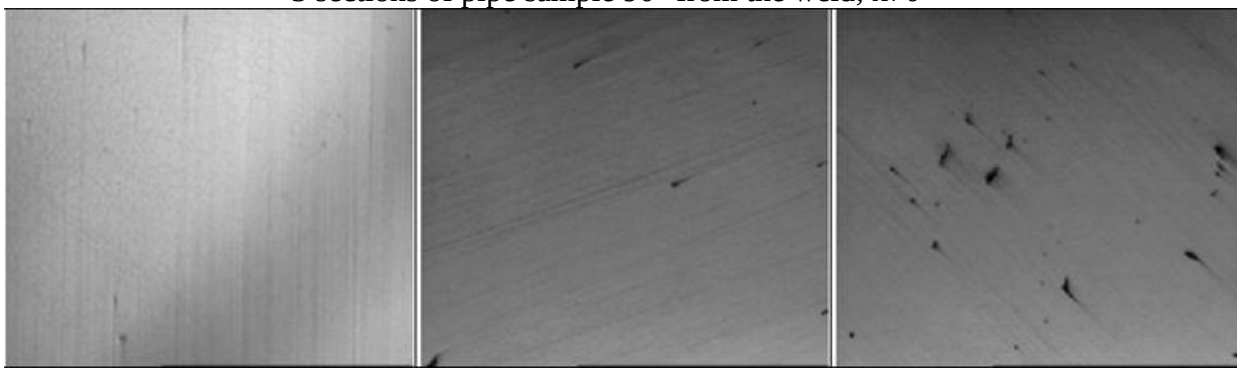

3 sections of pipe sample 180° from the weld; x70

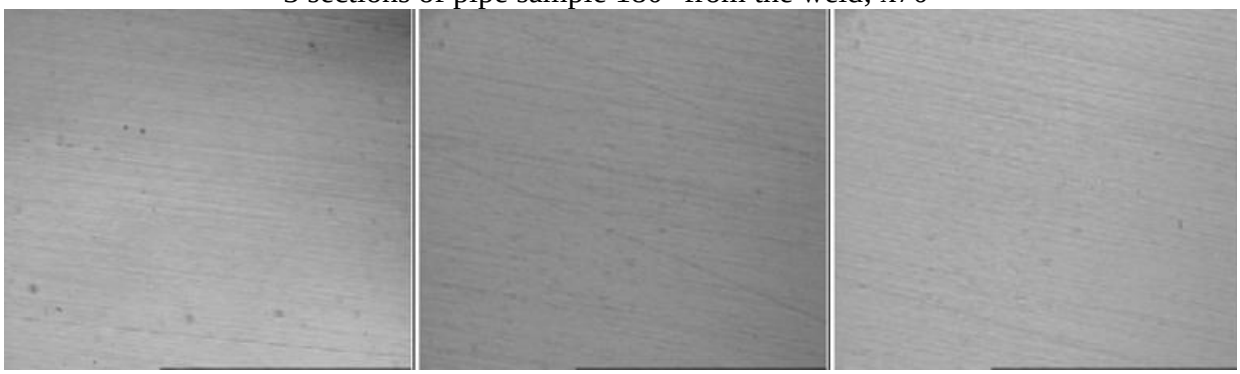

3 sections of pipe sample across the weld; x70

Figure 20. Micrographs of sections of a sample taken at 90°, 180° and across the weld after HIC testing taken at x70 magnification.

Dimensional Properties of Pipes

The forming and expansion parameters were controlled within a very narrow range and hence the end-to-end variation in pipe ovality (local and global) and internal diameter was negligible, Figure 21.

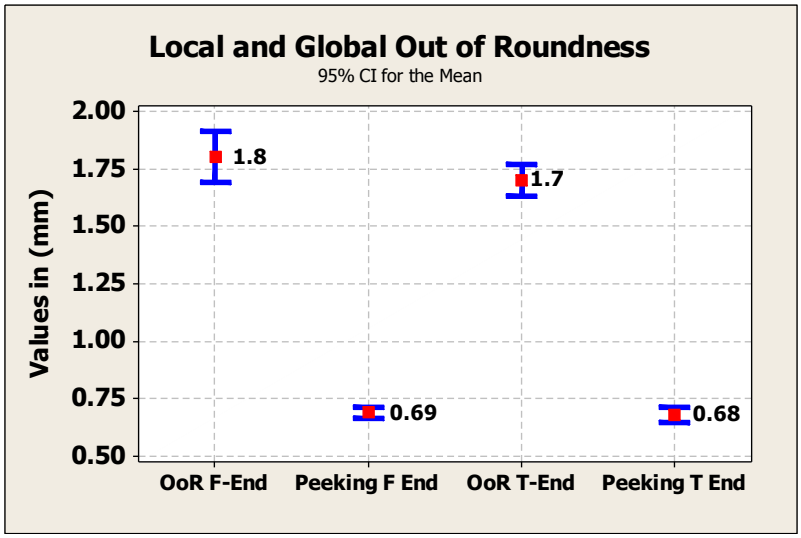

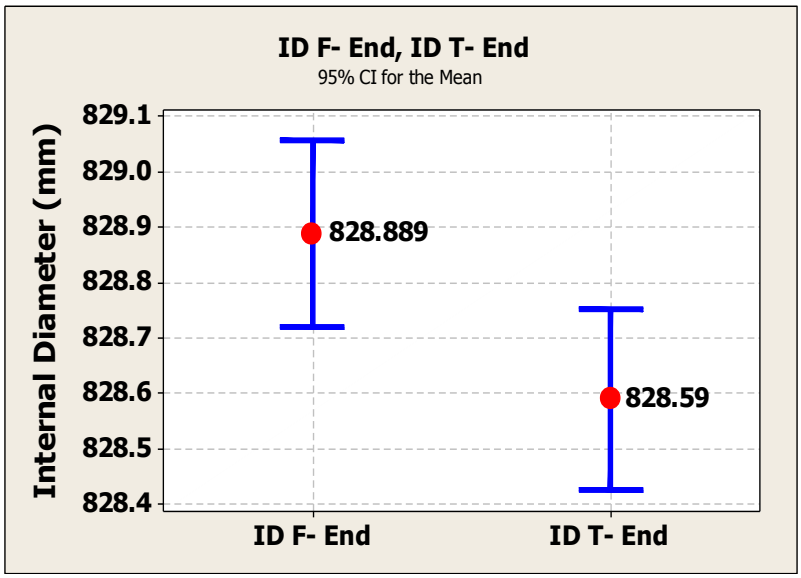

F-END: Front End of the Pipe; T-END: Trailing End of the Pipe

Figure 21. Pipe out-of-roundness and internal diameter.

Conclusions

The selection of alloy design and processing route for plate production routes, such as TMCP with accelerated cooling, is the key to attaining the desired microstructure throughout the plate thickness. The plate microstructure determines the plate properties and its behavior during pipe manufacturing and is a key to achieving enhanced and consistent HIC test results.

It is very important to select a narrow band of mechanical properties in plates for this D/t (~21) ratio as there are changes in mechanical properties after converting plates into pipes. These properties include strength, impact toughness and shear fracture area in drop weight tear tests.

It is very important to select the correct dimensions of the tools and crimping dies for edge crimping and JCO pipe forming to get better control of the pipe dimensional parameters starting from edge crimping, JCO forming and continuous tack welding. The correct forming process will reduce spring back and associated increase in residual stresses.

Also, the selection of pipe forming parameters, such as the number of strokes in the JCO press and percentage of expansion during mechanical expansion, plays an important role in managing residual stresses.

The selection of proper weld geometry for the weld groove design for ID and OD welding is required to avoid crack generation in the welding operation, mainly at the center of the weld seam.

The selection of pipe pre-heating temperature, welding consumables and welding parameters, such as speed, heat input and narrow gap weld geometry, are the main factors affecting toughness of the HAZ, weld, and hardness of the HAZ and weld plus HIC test results.

All above factors contribute to the ability of Welspun Corp Ltd-India to develop thick wall API5LX65MSO/L450MSO PSL2 linepipes for offshore sour service application.

References

1. I. Chattoraj, "The Effect of Hydrogen Induced Cracking on the Integrity of Steel Components," *Sadhana,* 20, (1) (February 1995), 199-211.

2. W.M. Hof et al., "New High Strength Large Diameter Pipes Steels," *Journal of Materials Engineering,* 9 (2) (1987), 191-198.

3. Ozgur Yavas, "Effect of Welding Parameters on the Susceptibility to Hydrogen Cracking in Line Pipe Steels in Sour Environments" (MS thesis, Metallurgical and Materials Engineering, The Graduate School of Natural and Applied Sciences, Middle East Technical University, December 2006).